IOP Conf. Series: Materials Science and Engineering **292** (2018) 012053 doi:10.1088/1757-899X/292/1/012053

Improvement in hydrogen storage properties of MgH_2 catalyzed with $BaTiO_3$ additive

J S Wang[1, 3, 4], W Zhang[1], S M Han[1, 2] and F Qin[3]

[1] State Key Laboratory of Metastable Materials Science and Technology, Yanshan University, Qinhuangdao 066004, PR China
[2] College of Environmental and Chemical Engineering, Yanshan University, Qinhuangdao 066004, PR China
[4] E-mail: bluceking@163.com

Abstract. The MgH_2+20 wt. % $BaTiO_3$ composites is prepared by ball milling MgH_2 with 20 wt. % $BaTiO_3$, and the effect of $BaTiO_3$ on the hydrogen storage properties of the MgH_2 is investigated. TPD (Temperature-programmed-desorption) results showed that with addition of $BaTiO_3$, the onset dehydrogenation temperature of the composite is 270 ^oC, which is 149 ºC lower than that of pure MgH_2. And the hydrogen absorption / desorption rates of MgH_2 + 20 wt.% $BaTiO_3$ are 2.21 times and 2.12 times of pure MgH_2 at certain temperatures and hydrogen pressures, respectively. Furthermore, $BaTiO_3$ additives decreased the dehydriding activation energy of MgH_2 from 116 kJ /mol to 108 kJ /mol. $BaTiO_3$ plays an effective catalyst role in the hydrogenation / dehydrogenation process of MgH_2.

1. Introduction

Hydrogen as a high density energy carrier has been attached great importance on its clean and inexhaustible properties [1]. The application of hydrogen needs a support from high capacity storage materials, such as MgH_2, which shows a high hydrogen storage capacity of 7.6 wt.% [2, 3]. However, MgH_2 suffers from high dehydrogenation temperature and poor kinetics, which limit its commercial application [4, 5].

In order to improve the hydrogen storage properties of MgH_2, many kinds of additives has been reported to be doped into MgH_2, such as transitional elements (Ti, V, Nb et al.) [6, 7], transition metal oxides [8], borides [9], fluorides [10, 11] and sulfides [12-14]. Barkhordarian et al. [15] and Hanada et al. [16] reported the remarkable improvement of hydrogen sorption kinetics by ball milling certain contents of Nb_2O_5 and MgH_2, and the studies of Ma et al. [17, 18] further certified that the Nb crystals distributed in the composites can work as the gateway to facilitate hydrogen transportation, and result in an improvement of the hydrogen storage properties of MgH_2. In recent years, Ti-based catalysts, including Ti, TiO_2, $TiCl_3$, TiF_3, were employed to decrease the desorption temperature of MgH_2 [19, 20]. When ball milled with MgH_2, the titanium oxides were found to result in significantly effects on reducing the onset dehydrogenation temperature of MgH_2, and increased the hydrogenation and dehydrogenation rates [21].

More recently, metal composite oxides [22, 23], were used as catalysts to improve the hydrogen storage properties of MgH_2. Baricoa et al. [24] investigated the effects of doping a perovskite-type $BaRuO_3$ into MgH_2, and reported that not only the RuO_6 octahedral structure could be penetrated by H_2, but the $BaRuO_3$ could destabilize MgH_2, which decreased the dehydrogenation temperature of

MgH_2. Besides, our group found that with 20 wt.% addition of $MgTiO_3$, the hydrogen storage performances of MgH_2 were remarkably improved [25].

In this paper, in consideration of the excellent catalytic effects of perovskite-type oxides and Ti-based additives, and the beneficial effect of perovskite-type structure compound on the diffusion of H_2 as mentioned above, a Ti-based perovskite-type $BaTiO_3$ was adopted as catalysts to further improve the hydrogenation/dehydrogenation properties of MgH_2. The effect of $BaTiO_3$ on the hydrogenation/dehydrogenation properties are studied, and more importantly, the effect mechanism is elucidated.

2. Experimental methods

The initial materials MgH_2 (98 %) and $BaTiO_3$ (99.5 %) were commercially purchased from Sigma-Aldrich. The MgH_2 powder was mixed with 20 wt.% $BaTiO_3$ powder which was mechanically milled for 2 h using a QM-ISP2 planetary, repeating 30 min milling and 15 min rest, with 500 $r \cdot min^{-1}$ under Ar atmosphere. The ball to powder weight ratio was about 40:1. All the sample manipulation was performed in an Ar-filled glove box to prevent getting in touch with oxygen and moisture.

The effect of $BaTiO_3$ addition on the dissociation temperature of the pure MgH_2 during the dehydrogenation was investigated by the temperature programmed desorption (TPD) apparatus. The hydrogen absorption/desorption kinetics of the samples was measured using a pressure-composition-temperature (P-C-T) characteristic measurement apparatus. Hydrogen absorption and desorption measurements were performed at desired temperature, with an initial hydrogen pressure of 3.0 MPa, and 0.1 MPa initial hydrogen pressure was given for the hydrogen desorption.

Samples after mechanical grinding and after hydriding/dehydriding cycling were characterized by X-ray diffraction (XRD) with Cu Kα radiation , using D/MAX-2500/PC, The 2θ angle was varied from 10° to 80°. Hydrogen desorption properties were investigated by a simultaneous thermal analyzer (DTG-60A) under flowing Ar at a rate of 100 $mL \cdot min^{-1}$, which were rising from room temperature to 500 °C with a heating rate of 5, 10, 15 and 20 $^{o}C \cdot min^{-1}$.

3. Results and discussion

3.1. Hydrogen absorption/desorption performances

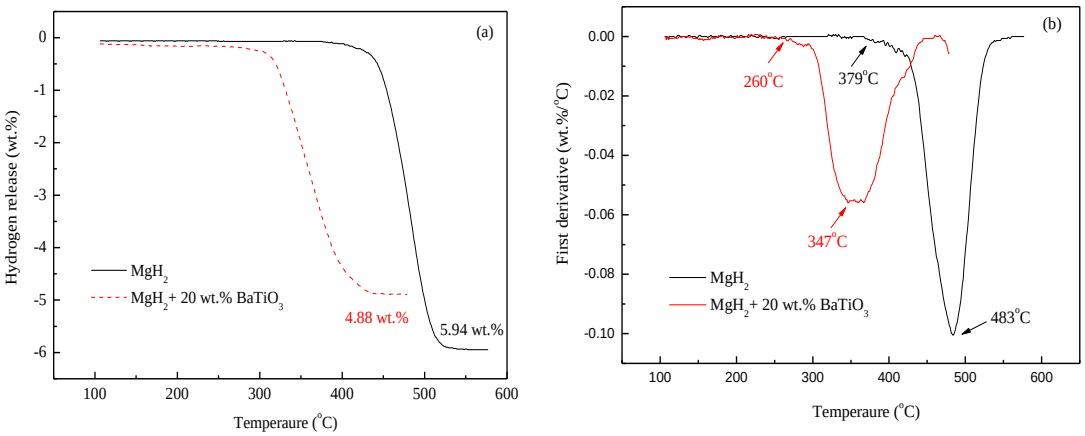

Figure 1. TPD curves of MgH_2 and MgH_2+20 wt. % $BaTiO_3$.
(a) Temperature-desorption contents curves; (b) The first derivative curves of (a).

Figure1 presents the dehydrogenation curves of the MgH_2+20 wt.% $BaTiO_3$ and the pristine MgH_2 when they are heated from 100 ºC to 550 ºC at a rate of 10 $ºC \cdot min^{-1}$. The pristine MgH_2 starts to release hydrogen at about 389 ºC, with a hydrogen desorption capacity of about 5.94 wt.%. In case of MgH_2+20 wt.% $BaTiO_3$, the onset dehydrogenation temperature is 260 ºC, and the peak temperature is 347 ºC, 119 ºC and 136 ºC lower than that of pure MgH_2, respectively, and its total dehydrogenation amount reaches 4.88 wt.% by 433 ºC. Obviously, the addition is effective to improve the thermal

decomposition characteristics of MgH_2 with results of decreasing desorption temperature. As for the maximum hydrogen release content, it seems that MgH_2+20 wt.% $BaTiO_3$ decreased almost 1wt.% than that of pure MgH_2. However, it should be noticed that the 20 wt.% $BaTiO_3$ additives were not hydrogen absorption materials. Thus, the maximum hydrogen desorption amount was shown relatively less in the diagram.

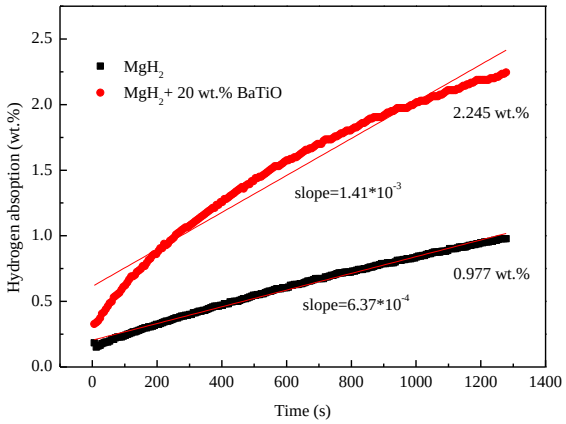

Figure 2. Comparison of the absorption kinetics of MgH_2 and MgH_2+20 wt. % $BaTiO_3$.

Figure 2 presents the hydrogen absorption curves of the received MgH_2 and the MgH_2+20 wt.% $BaTiO_3$ at 150 °C under 3 MPa hydrogen pressure. It should be noticed that all the samples are measured after two hydrogen absorption/desorption cycles. The representative curve shows that the received MgH_2 absorbs only 0.977 wt. % hydrogen within 21 min, whereas under identical conditions, MgH_2+20 wt. % $BaTiO_3$ absorbs 2.245 wt. % hydrogen, almost 2.3 times of pure MgH_2. Furthermore, the linear fitting of above isothermal desorption curves shows that for the MgH_2+20 wt. % $BaTiO_3$ sample, the average diffusion rate of H at 150 °C is $1.41*10^{-3}$ wt.%/s, and the value for pure MgH_2 is $6.37*10^{-4}$ wt.%/s. The results illustrate at 150 °C, the hydrogen absorption rate of MgH_2+20 wt. % $BaTiO_3$ is almost 2.21 times of pure MgH_2. It is obvious that the addition of $BaTiO_3$ significantly accelerates the hydrogen absorption rate of MgH_2.

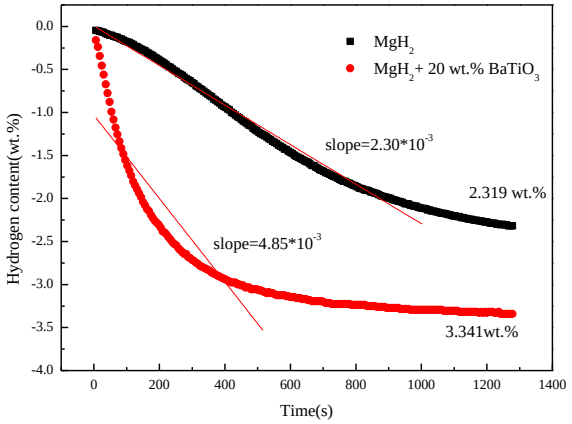

Figure 3. Comparison of the desorption kinetics of MgH_2 and MgH_2+20 wt. % $BaTiO_3$.

The isothermal dehydrogenation curve for MgH_2 samples with and without 20 wt. % $BaTiO_3$ at 350 ºC are shown in figure 3. Within 21 min, 2.319 wt. % hydrogen was dehydrogenated for MgH_2. As for the MgH_2+20 wt. % $BaTiO_3$ composites, 3.341 wt. % hydrogen was dehydrogenated under the same condition, which was about 1.44 times than that of pure MgH_2. And for the MgH_2+20 wt. % $BaTiO_3$, releasing 90% hydrogen takes only 500 seconds, while it takes more than 1000s for pure MgH_2. According to the fitting curve, at 350 ºC, the dehydrogenation rate of MgH_2+20 wt. % $BaTiO_3$ is $4.85*10^{-3}$ wt.%/s, almost 2.12 times of pure MgH_2. Therefore, with the introduction of 20 wt.%

$BaTiO_3$, not only the hydrogen absorption rate of MgH_2, but also the hydrogen desorption rate can be remarkably improved.

3.2. Activation energy for decomposition of the MgH_2-$BaTiO_3$ composite

The hydrogen desorption kinetics curves of pristine MgH_2 and MgH_2-$BaTiO_3$ composites at different heating rates are shown in figure 4. After doping $BaTiO_3$, the decomposition temperature of the samples is obviously decreased. At a heating rate of 10 °C/min, in compared with pure MgH_2, the dehydrogenation peak temperature is lowered by 43 °C for MgH_2+20 wt. % $BaTiO_3$.

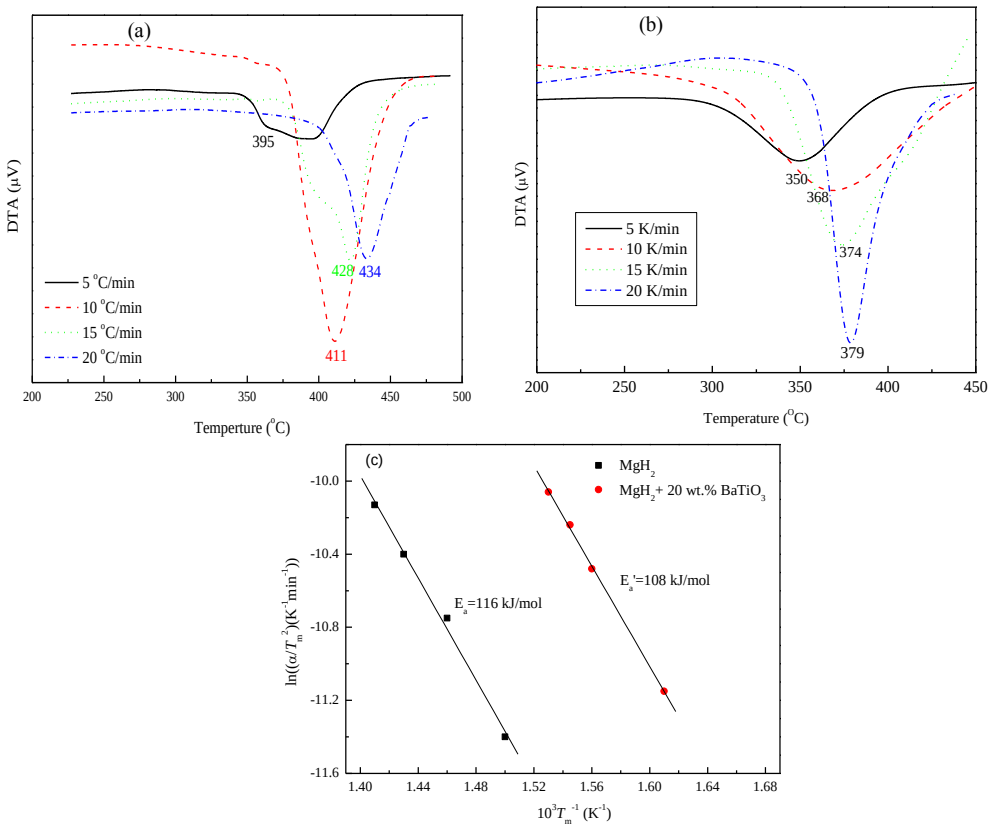

Figure 4. DTA curves of different sample at various heating rates
(a) MgH_2; (b) MgH_2+20wt. % $BaTiO_3$; (c) Kissinger's plots.

In order to understand the fast hydrogen desorption kinetics, the activation energy of the dehydrogenation process for the pure MgH_2 and the MgH_2-$BaTiO_3$ was estimated with Kissinger's method [26].

$$\frac{d\left[Ln\left(\alpha/T_m^{\,2}\right)\right]}{d\left[1/T_m\right]} = -\frac{E_a}{R} \qquad (1)$$

Where α is the heating rate, Tm is the absolute temperature at the maximum desorption rate, and R is the ideal gas constant. The activation energies of different composites were evaluated by the DTA using Kissinger formula. Figure4 (c) shows Kissinger plots for the desorption reaction of MgH_2+20 wt.% $BaTiO_3$. The activation energy value is 116 kJ/mol and 108 kJ/mol for pristine MgH_2 and MgH_2+20 wt.% $BaTiO_3$ composite, respectively. The calculated results show that $BaTiO_3$ additives decrease activation energy during dehydriding, and therefore improve the dehydriding rate of the composite.

3.3. Structural characterization and effect mechanism of the MgH_2-$BaTiO_3$ composite

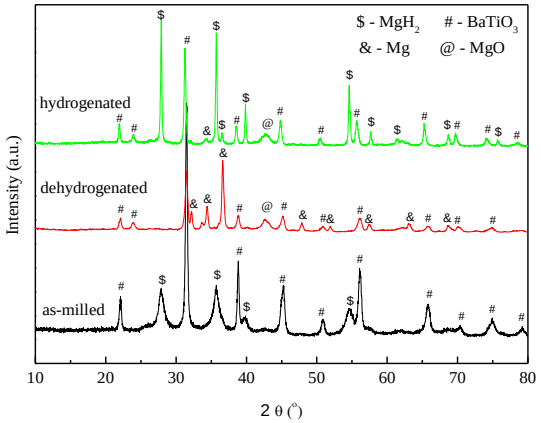

Figure 5. XRD patterns of MgH_2-$BaTiO_3$ composite.

The XRD patterns of the MgH_2 with 20 wt. % $BaTiO_3$ are shown in figure 5. For the dehydrogenated sample, MgH_2 phase is replaced by Mg phases, and a weak peak corresponding to MgO is found in both the dehydrogenated and the hydrogenated patterns, which is due to the oxidation of Mg when transferring the dehydrogenated sample during the test process. Furthermore, the results shows that $BaTiO_3$ remains stable after ball-milling, hydriding and dehydriding processes, indicating that there are no reaction between $BaTiO_3$ and MgH_2, but $BaTiO_3$ play a catalyst role during the hydriding/dehydriding process of MgH_2, which result in the decrease in desorption temperature and improvement in kinetics of MgH_2. According to the research results of Lin et al., the Ti-based catalysts owing to special electron distribution help in particle transfer in chemical reactions and have been applied in many chemical processing [27]. Therefore, $BaTiO_3$ play a catalytic role in the hydrogenation/dehydrogenation reactions of MgH_2, which helps to improve the hydrogen storage properties of MgH_2.

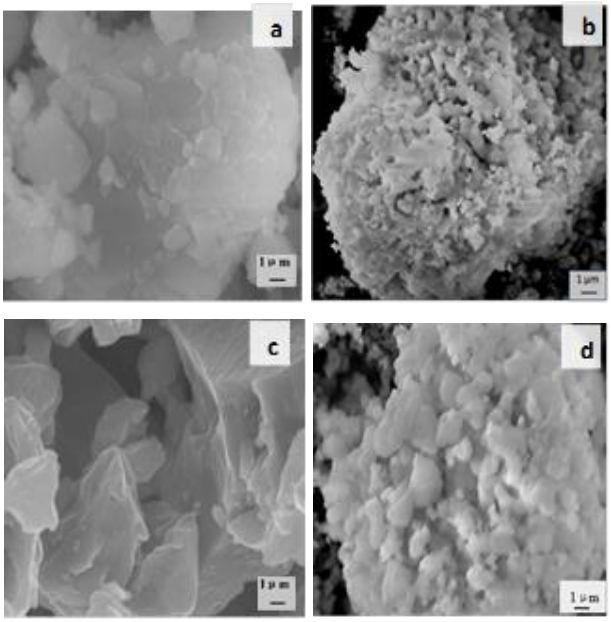

Figure 6. SEM morphology of the: (a) MgH_2 as-milled; (b) MgH_2 + 20 wt.% $BaTiO_3$ composite as-milled; (c) MgH_2 after hydrogenation; (d) MgH_2 + 20 wt.% $BaTiO_3$ composite after hydrogenation.

In order to futher study the microstructure and effect mechanism of the composite, Scanning Electron Microstructure is exploited to characterize the samples after ball-milling and hydrogenation

process. As shown in figure 6, for the as-milled samples, the particle sizes of the MgH_2+20 wt.% $BaTiO_3$ shows a smaller and more homogeneous particle size compared to pure MgH_2. In addition, the average particle size of MgH_2+20 wt.% $BaTiO_3$ is also found to be smaller than that of pure MgH_2 after hydrogenation processes.That illustrates the addition of $BaTiO_3$ to MgH_2 can reduce the degree of aggregation of the particles during the ball-milling and the hydrogenation process. As reported by Peng et al.cx [28], smaller size particle and fewer amounts of clusters inside the hydrogen storage materials can facilitate hydrogenation/ dehydrogenation kinetics due to more H diffusion channels in the matrix. Therefore, by doping $BaTiO_3$ into the MgH_2, we're able to make uniform and homogeneous microstructures that have more remarkable hydrogen storage properties compared to pure MgH_2.

4. Conclusions

The thermodynamic and kinetic properties of MgH_2+ 20wt.% $BaTiO_3$ are investigated. In comparison with the pure MgH_2, the onset desorption temperature of the MgH_2+20 wt. % $BaTiO_3$ composite decreased about 119 ^oC, and the hydrogen absorption capacity increased by 2.3 times at 150 ^oC, the desorption capacity increased by 1.44 times at 350 ^oC within 21 min. According to DTA results measured at different heating rate, activation energy of composites decreased from 116 kJ/mol to 108 kJ/mol for MgH_2+20 wt. % $BaTiO_3$. $BaTiO_3$ play a catalytic role in the hydriding / dehydriding of MgH_2, which is responsible for the hydrogen storage properties improvement of MgH_2.

Acknowledgments

This work was financially supported by the National Natural Science Foundation of China (NOs.51571173 and 21606193), China Postdoctoral Science Foundation (2016M601281), and the Fundamental Research Funds for the Central Universities (Grant No. 3142015009).

References

[1] Pei L C, Han S M, Wang J S, Hu L, Zhao X and Liu B Z 2012 *Mater Sci Eng B* **177** 1589
[2] Kurko S, Milanović I, Grbović Novaković J, Ivanović N and Novaković N 2014 *Int. J Hydrogen Energy* **39** 862
[3] Floriano R, Leiva D R, Deledda S,Hauback B C and Botta W J 2014 *Int. J Hydrogen Energy* **39** 4404
[4] Shimada M, Higuchi E and Inoue H 2013 *J. Alloys Compd* **580** Supplement 1 S153
[5] Leng H Y, Pan Y B, Li Q and Chou K C 2014 *Int. J. Hydrogen Energy* **39** 13622
[6] Charbonnier J, Rango P D, Fruchart D et al. 2004 *J. Alloys Compd* **383** 205
[7] Rivoirard S, Rango P D, Fruchart D, Charbonnier J and Vempaire D 2003 *J. Alloys Compd* **Supplement 356–357** 622
[8] Floriano R, Leiva D R, Deledda S, Hauback B C and Botta W J 2013 *Int. J. Hydrogen Energy* **38** 16193
[9] Liu G,Qiu F, Li J, Wang Y,Li L, Yan C, Jiao L and Yuan H 2012 *Int. J. Hydrogen Energy* **37** 17111
[10] Jin S A, Shim J H, Cho Y W and Yi K W 2007 *J. Power Sources* **172** 859
[11] Zhang J, Huang Y N, Mao C and Peng P 2012 *J. Alloys Compd* **538** 205
[12] Jia Y H, Han S M, Zhang W, Zhao X, Sun P F, Liu YQ, Shi H and Wang J S 2013 *Int. J. Hydrogen Energy* **38** 2352
[13] Wang J S, Zhang W, Cheng Y, Ke D D and Han S M 2015 *J. Wuhan University of Technology-Mater. Sci. Ed* **30** 670
[14] Zhang W, Cheng Y, Han D and Han S M 2015 *Energy* **93** 625
[15] Barkhordarian G, Klassen T, Bormann R 2006 *J. Alloy. Compd* **407** 249
[16] Hanada N, Ichikawa T, Hino S and Fujii H 2006 *J. Alloy. Compd* **420** 46
[17] Ma T, Isobe S, Morita E, WangY, Hashimoto N, Ohnuki S, Kimura T, Ichikawa T and Kojima Y 2011 *Int. J. Hydrogen Energy* **36** 12319
[18] Ma T, Isobe S, Wang Y, Hashimoto N and Ohnuki S 2013 *J. Phys. Chem. C* **117** 10302

[19] Shahi R R, Bhatnagar A, Pandey S K, Dixit V and Srivastava O N 2014 *Int. J. Hydrogen Energy* **39** 14255
[20] Ren C, Fang Z Z, Zhou C, Lu J, RenY, Zhang X and Luo X 2014 *Int. J. Hydrogen Energy* **39** 5868
[21] Croston D L, Grant D M and Walker G S 2010 *J. Alloys Compd* **492** 251
[22] Xu G, Shen N, Chen L J, Chen Y and Zhang W 2017 *Mater. Res. Bull.* **89** 197
[23] Shan J W, Li P, Wan Q, Zhai F Q, Zhang J, Li Z L, Liu Z J, Volinsky A A and Qu X H 2014 *J. Power Sources* **268** 778
[24] Baricco M, Rahmana M W, Livraghia S, Castelleroa A, Enzob S and Giamello E 2012 *J. Alloy. Compd* **536** S216
[25] Wang J S, Han S M, Li Y, Shen N and Zhang W 2014 *Acta Physico-Chimica Sinica* **30** 2323
[26] He K 1957 *Anal. Chem*, **29** 1417
[27] Lin H J, Ouyang L Z, Wang H, Zhao D Q, Wang W H, Sun D L and Zhu M 2012 *Int. J. Hydrogen Energy* **37** 14329
[28] Peng S K, Xiao X Z, Xu R J, Li L, Wu F, Li S Q, Wang Q D and Chen L X 2010 *T Nonferr Metal Soc* **20** 1879